5-11-2002

The Design and Implementation of a Yield Monitor for Sweetpotatoes

Swapna Gogineni

THE DESIGN AND IMPLEMENTATION OF A YIELD MONITOR FOR SWEETPOTATOES

By

Swapna Gogineni

A Thesis
Submitted to the Faculty of
Mississippi State University
in Partial Fulfillment of the Requirements
for the Degree of Master of Science
in Electrical Engineering
in the Department of Electrical and Computer Engineering

Mississippi State, Mississippi

May 2002

THE DESIGN AND IMPLEMENTATION OF A YIELD MONITOR FOR SWEETPOTATOES

By

Swapna Gogineni

Approved:

J. Alex Thomasson Associate Professor of Agricultural and Biological Engineering (Director of Thesis)	Nicholas H. Younan Professor of Electrical and Computer Engineering (Major Advisor and Graduate Coordinator)
Robert J. Moorhead Professor of Electrical and Computer Engineering (Committee Member)	Wayne Bennett Dean of the College of Engineering

Name: Swapna Gogineni

Date of Degree: May 11, 2002

Institution: Mississippi State University

Major Field: Electrical Engineering

Major Professor: Dr. Nicholas H. Younan

Title of Study: THE DESIGN AND IMPLEMENTATION OF A YIELD MONITOR FOR SWEETPOTATOES

Pages in Study: 62

Candidate for Degree of Master of Science

A study of the soil characteristics, weather conditions, and effect of management skills on the yield of the agricultural crop requires site-specific details, which involves large amount of labor and resources, compared to the traditional whole field based analysis. This thesis discusses the design and implemention of yield monitor for sweetpotatoes grown in heavy clay soil. A data acquisition system is built and image segmentation algorithms are implemented. The system performed with an R^2 value of 0.80 in estimating the yield. The other main contribution of this thesis is to investigate the effectiveness of statistical methods and neural networks to correlate image-based size and shape to the grade and weight of the sweetpotatoes. An R^2 value of 0.88 and 0.63 are obtained for weight and grade estimations respectively using neural networks. This performance is better compared to statistical methods with an R^2 value of 0.84 weight analysis and 0.61 in grade estimation.

ACKNOWLEDGEMENTS

I would like to primarily thank Dr. Alex Thomasson, my research advisor, for giving me the opportunity to work on this project, and guiding me throughout this work and for providing financial support for my Masters degree. I would also like to thank Dr. Younan and Dr. Moorhead for their valuable comments and suggestions. I would like to thank Mr. James Wooten for his guidance and assistance throughout the project and helping me with the statistical methods and GIS tools used in the project.

TABLE OF CONTENTS

CHAPTER Page

LIST OF TABLES

LIST OF FIGURES

FIGURE Page

FIGURE Page

CHAPTER I

INTRODUCTION TO YIELD MONITORING

1.1 Overview

Yield monitoring is a process of measuring and mapping the site-specific yield of agricultural crops to study the effects of soil characteristics, weather conditions, and management on production [1]. The advent of sophisticated technologies like remote sensing and machine vision have laid the path for yield and quality monitoring of crops, which can facilitate maximizing the harvest production and making efficient use of fertilizers [1]. Sensors are used to measure yield, which is combined with information obtained from a Global Positioning System (GPS) receiver to generate yield maps [2].

Sweetpotato acreage in northeast Mississippi recently increased by 113%, and the value of production increased from $8,000,000 to $19,000,000 [3]. Yield monitors that have been developed for sweetpotatoes utilize the measured weight of the crop traveling over the conveyor belt to analyze the yield [4, 5]. This procedure was successful for sweetpotatoes grown in sandy soil but failed to monitor yield for sweetpotatoes grown in Mississippi. The heavier clay soil in Mississippi sweetpotato fields results in large lumps of soil on the conveyor belt, increasing the estimated weight and leading to misinterpretation [6]. To overcome this problem, a machine vision approach can be used for yield monitoring of sweetpotatoes [6]. Today, grading of sweetpotatoes

in Mississippi is performed by hand picking the sweetpotatoes from the conveyor belt and separating them according to their shape and size. This approach results in a high cost of labor, errors in detection, inconsistency in grading, and low efficiency. An automated instrument will result in benefits by reducing the cost and increasing the efficiency.

1.2 Previous Investigations

Many manufactures like Ag Leader, John Deere, etc. have developed commercial yield monitors for agricultural crop. Different measurement techniques have been used to monitor yield. HarvestMaster developed a yield monitor for potatoes that used load cells to estimate the yield [5]. This technique fails for Mississippi-grown sweetpotatoes that are grown in clay and clay loam soils. This technique also has a drawback of providing only weight estimates of the yield and does not provide any information of the yield of each grade of sweetpotatoes in the field. The problem of yield and grade monitoring of sweetpotatoes has not been solved, and no appropriate commercial device is available for Mississippi farmers.

Machine vision has been used in the past to solve various problems in agriculture. Deck et. al attempted grading of potatoes with the help of neural networks in 1992 [7]. Potatoes were allowed to travel on a conveyor belt. Two images of potatoes were taken at right angles to each other. These images were used to detect defects in potatoes. Linear discriminant analysis and neural networks were used for grading and detecting defects.

In 1995, Searcy and Alchanatis developed a system for high-speed inspection of carrots [8]. Image processing and neural networks were used to accomplish the task of

detecting defects in carrots. Irregular surfaces of the carrots were considered to be defects. Neural networks were later on used to detect defects in the color of the carrots.

Delwiche et. al developed a high-speed sorting system for dried prunes using machine vision [9]. Images of dried prunes were taken with three cameras. A black background was used to increase the contrast. Intensity gradient was used to differentiate bad prunes from good ones. Many more examples can be cited where machine vision is used in grading and detection of objects from vegetables, fruits, seeds, and wood chips to eggs [10, 11].

Machine vision was not only used in detecting and grading vegetables and seeds, but was also used in the mining industry. Crida and Jagar used an active vision approach to recognize and measure the distribution of a rock's size [12]. This system was used in the gold mining industry to control and monitor the material being milled. The Hough transform was initially used to detect rocks and then multiscalar image pyramids were used for target detection [13].

1.3 Relationship with the Previous Work

In 1999, the Department of Agricultural and Biological Engineering at Mississippi State University came up with an algorithm to categorize sweetpotatoes according to their size [6]. A relationship between the image-based size and shape with the weight and grade of the sweetpotatoes was developed. For the analysis 10 nulls, 10 canners, 10 U.S. No.1's, and 6 jumbos were considered. Images of the sweetpotatoes were taken with a USB camera one sweetpotato at a time with a dark background. Features were extracted from these images with the sweetpotatoes manually painted

white. Weight correlation using linear-regression analysis performed with an R^2 of 0.9271. Table 1.1 shows the results that were obtained during grading of sweetpotatoes into different categories using dicriminant analysis. This study is an extension of the project and focuses on developing an automatic system for detection and estimation of grade and weight of the sweetpotatoes.

Table 1.1: Results of the accuracy of size classification based on image based size measurement of sweetpotatoes from the experiments carried out in 1999 [6].

Actual/Predicted	Null	Canner	U.S. No.1	Jumbo
Null	100%	0%	0%	0%
Canner	20%	80%	0%	0%
U.S. No.1	0%	0%	88.9%	11.1%
Jumbo	0%	0%	0%	100%

1.4 Summary

This thesis discusses the techniques developed for yield monitoring of sweetpotatoes grown in heavier clay soil. Figure 1-1 gives an overview of the machine vision system that is developed to estimate the yield. An image acquisition system that can be operated in harsh environments and consume low power is developed. Image segmentation algorithms with edge detection and texture information are developed to detect sweetpotatoes. Algorithms are developed for grading sweetpotatoes and estimating the weight. Finally images are processed to create yield maps with the help of spatial information from the global positioning system.

The main focus of the present research is to develop a machine vision system to monitor yield for sweetpotatoes. Chapter II explains various object identification techniques. Chapter III presents the image acquisition system that has been built. Chapter IV discusses the software design for the detection and grading of sweetpotatoes. Experiments and corresponding results have been presented in Chapter V and Chapter VI. Finally in Chapter VII, conclusions and future work for improvements are discussed.

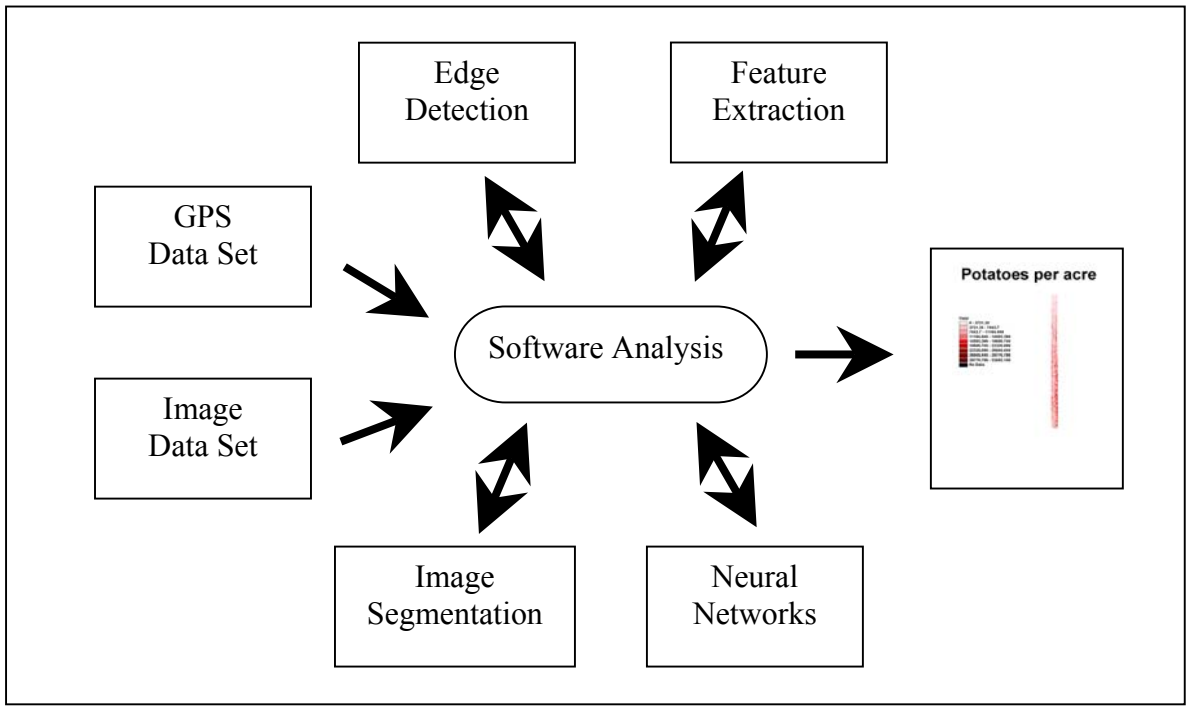

Figure 1-1: Overview of the approach used for yield monitoring of Mississippi-grown sweetpotatoes

CHAPTER II

THEORY

2.1 Sweetpotato Categories

For the purpose of this study, sweetpotatoes, which are plant roots are categorized into 4 categories: cull, canner, U.S. No.1, and Jumbo. Figure 2-1 shows the various categories of sweetpotatoes. This section discusses the classification of sweetpotatoes according to their sizes.

Cull

Culls are a grade of sweetpotatoes, that are distorted in shape, or damaged, or very small and are usually discarded during the harvest. The very small sweetpotatoes are called nulls. Typical examples of culls are sweetpotatoes that are long and thin, broken, or have a sharp curve at the center.

Canner

These sweetpotatoes are larger than nulls. Canners are 1 to 2 inches in diameter and 2 to 7 inches in length. They are suitable for sale to canneries, but are severely discounted in price.

(a) Cull (b) Canner

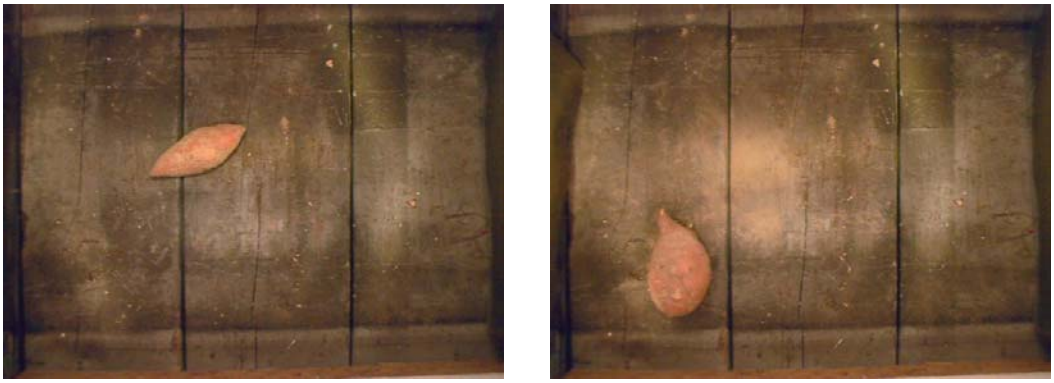

(c) U.S. No.1 (d) Jumbo

Figure 2-1: Sample images of the various grades of sweetpotatoes

U.S. No.1

U.S. No.1 sweetpotatoes are larger than canners and considered to be of highest quality. They are worth eight to nine times more than other grades; due to this reason, accurate grading is very important for U.S. No.1. These sweetpotatoes are 2 to 3.5 inches in diameter and 3 to 9 inches in length.

Jumbo

Jumbos are sweetpotatoes larger than U.S. No.1. Roots exceeding 3.5 inches in diameter or more than 9 inches in length fall in this category. Due to their large size, they are usually discarded or sold at a greatly discounted price. Various other sub-grades are present, which will not be considered for this work.

2.2 Image Segmentation Fundamentals

An image is a two dimensional representation with encoded information of one or more aspects like color, texture, depth, intensity, velocity, etc. It can be represented by a two dimensional function *f(x, y)*, where *(x, y)* denote the spatial coordinates and the amplitude of *f* at a given point is called the gray level [14]. Analog images must be digitized before performing any analysis. Each digital image consists of a finite number of elements called pixels. Figure 2-2 shows an example image taken during sweetpotatoes harvest. This image will be used for demonstrating various image segmentation techniques and algorithms.

In the analysis of the objects in images, it is essential to locate and identify the objects in the image. This process of partitioning an image into distinct non-overlapping regions is called image segmentation [15]. To identify objects in an image, segmentation is critical. Region growing is one approach to image segmentation in which neighboring pixels are analyzed and added to a region if no edge is detected. The remainder of this section provides background to popular image segmentation algorithms like gray level thresholding, edge detection, morphology, and Hough transform.

Figure 2-2: Sample image of a sweetpotato harvest

Gray Level Thresholding

Thresholding is the simplest approach in image segmentation. In this approach, pixels in an image are divided into various segments according to their gray level [14, 16]. Segmenting an image into two regions with thresholding is called a bi-level thresholding. A bi-level thresholding is given in equation (2.1). A multilevel thresholding is also possible by setting various threshold values. The difficulty lies in selecting a function to perform the thresholding and to select a proper threshold value. Gray level histograms can be used in selecting the threshold value.

$$\begin{aligned} g(i,j) &= 1 \quad \text{for } f(i,j) \geq T \\ &= 0 \quad \text{for } f(i,j) < T \end{aligned} \tag{2.1}$$

Edge Detection

Edge detection can be explained as an approach for detecting discontinuity in gray level in the image [16]. The discontinuity in gray level corresponds to the presence of an edge. Discontinuity in gray level can be present in any direction (east, west, north, south,

etc). The presence of noise in the image results in unwanted edges, which can be eliminated by choosing an appropriate cutoff for the magnitude of the calculated edge. Pixels with the edge magnitude greater than the cutoff correspond to the edge.

Many edge detectors, like Roberts, Sobel, Kirsch, and Laplacian operators, have been proposed to perform edge detection in a specified direction. The kirsch operator, on the other-hand, calculates the gradient in all directions and takes the maximum gradient into consideration. If this maximum gradient lies above the cutoff, then the pixel corresponds to the edge. Figure 2-3 shows 8 directions in which edges can be detected. Adding all the pixels multiplied with their respective weights produces the output magnitude.

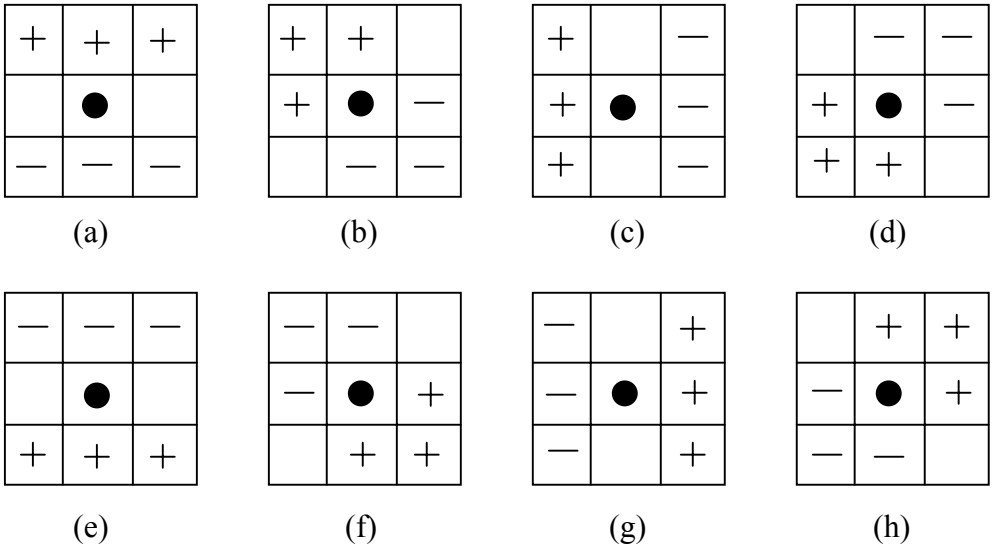

Figure 2-3: Various edge detection masks

Considering Figure 2-2(a), the magnitude is given by

$$g(x,y) = g(x-1,y-1) + g(x,y-1) + g(x+1,y-1) - g(x-1,y+1) - g(x,y+1) - g(x+1,y+1) \quad (2.2)$$

$$= \sqrt{g_x^2 + g_y^2} \quad (2.3)$$

The direction of the edge is given by

$$\theta = \tan^{-1}\left(\frac{g_x}{g_y}\right) \quad (2.4)$$

Morphology

Mathematical morphology in image processing is derived from *set theory*. Morphological operation can be explained as taking a structured element and applying it to each and every element in the image to obtain a desired shape [17]. Morphological operation can be used to get a better understanding of the features of the objects in the image. This section discusses two basic operations of mathematical morphology: Dilation and erosion.

Dilation can be defined as a process of enlarging the boundaries of the image. This process eliminates the holes in a region. Erosion can be defined as the reverse process. In erosion, the boundaries of the object shrink and holes if present are enlarged. Other processes like closing, opening, and medial axis transform are also categorized as morphological operations.

Hough Transform

The Hough Transform is a technique of identifying a particular shape in an image [18, 19]. The Hough transform is particularly helpful in detecting shapes like straight lines, circles, ellipse, curves, etc. A straight line at a distance r and inclination θ ranging from $[0,\pi]$, can be represented in a parametric space by

$$r = x\cos\theta + y\sin\theta \tag{2.5}$$

Therefore, the Hough transform of a straight line becomes a point and the Hough transform of a point becomes a curve in the parametric space. The lines in an image are found by transforming all the points in the *x*-*y* plane to the $r-\theta$ plane. The peaks in the $r-\theta$ plane correspond to the straight line in the *x*-*y* plane. Similar procedures can be followed to identify circles in the image with

$$(x-x_0)^2 + (y-y_0)^2 = r^2 \tag{2.6}$$

where (x_0, y_0) corresponds to the center of the circle and *r* is the radius. An ellipse, on the other-hand, can be represented as

$$\frac{(x-x_0)^2}{a^2} + \frac{(y-y_0)^2}{b^2} = 1 \tag{2.7}$$

where *a* and *b* correspond to the radial distance in the *x* and *y* direction.

Taking into consideration the orientation, θ, of the ellipse, a more general form can be used for representing equation (2.7). That is:

$$\begin{pmatrix} x-x_0 \\ y-y_0 \end{pmatrix} = \begin{pmatrix} a\cos\theta\cos\phi + b\sin\theta\sin\phi \\ b\cos\theta\sin\phi - a\sin\theta\cos\phi \end{pmatrix} \tag{2.8}$$

2.3 Polar Moment of Inertia

The image-based size and shape plays a major role in the grading of sweetpotatoes. Many algorithms were proposed in the past that used the knowledge of the shape of an object to predict its size. The polar moment of inertia in this scenario helps to some extent [20]. Mass is a measure of how readily an object accelerates due to a given force. The moment of inertia of an object measures how easily an object rotates about an axis of rotation. Thus, objects with larger moments of inertia about an axis will be harder to rotate with a set amount of torque. Considering an object in 2 dimensions, circular objects can be rotated with less torque then compared to object of other shapes. Thus the polar moment of inertia increases with an increase in the size and the elongation of the object.

The moment of inertia of an area A, as shown in Figure 2-4, with respect to the x and y axis can be defined as follows.

$$I_x = \int_A y^2 dA \tag{2.9}$$

$$I_y = \int_A x^2 dA \tag{2.10}$$

Representing x and y in polar coordinates yields

$$x = \rho \cos\theta \tag{2.11}$$

$$y = \rho \sin\theta \tag{2.12}$$

$$\rho^2 = x^2 + y^2 \tag{2.13}$$

$$\theta = \tan^{-1}\left(\frac{y}{x}\right) \tag{2.14}$$

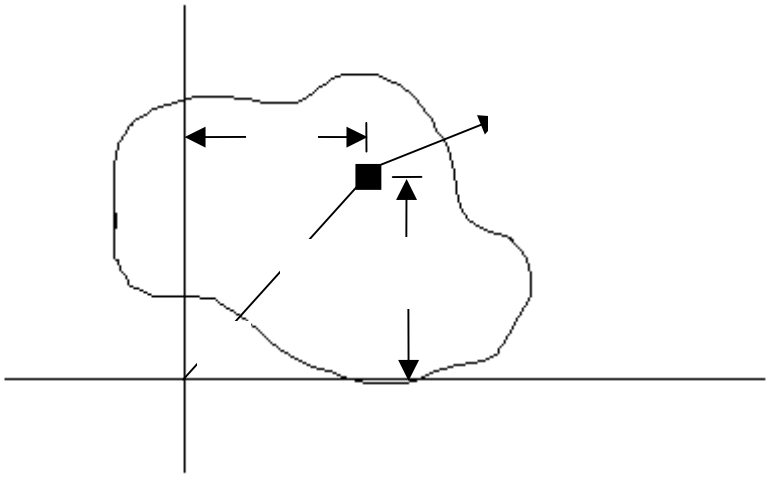

Equations (2.9) and (2.10) are the rectangular moments of inertia. The moment of inertia in the polar coordinates can be represented as

$$J_o = \int_A \rho^2 dA \tag{2.15}$$

$$\rho^2 = x^2 + y^2 \tag{2.16}$$

then,

$$J_o = \int_A (x^2 + y^2) dA \tag{2.17}$$

$$= \int_A x^2 dA + \int_A y^2 dA \tag{2.18}$$

$$= I_x + I_y$$

2.4 Weight and Grade Estimation

Two types of information are important in building a map for sweetpotatoes; the weight of the sweetpotatoes and the grade of sweetpotatoes. Grading of sweetpotatoes is done on the basis of their shape and size, which was discussed in section 2.1. This section will discuss various procedures that will be used in the weight and grade estimation.

Statistical Methods

As mentioned in Section 1.3, Wooten et al. used REG and DISCRIM procedures to estimate the weight and the size of the sweetpotatoes images that were manually painted white [6]. The pixel area covered by the sweetpotato along with the polar moment of inertia was extracted. This study will compare the performance of these statistical methods to neural networks.

The REG Procedure

The REG procedure fits linear regression models by least squares [21, 22]. In general terms, linear regression tries to fix a straight line that best predicts the output from the input by minimizing the deviation of the sum of squares. In simple linear regression the output Y, can be predicted from the input X, as given below

$$Y_i = \beta_0 + \beta_1 X_i + \varepsilon_i \tag{2.19}$$

In polynomial regression the output Y, can be predicted by a polynomial function of a regressor variable X. Equation 2.20 shows the polynomial regression

$$Y_i = \beta_0 + \beta_1 X_i + \beta_2 X_i^2 + \varepsilon_i \tag{2.20}$$

Given a variable *Y*, which can be predicted using a linear combination of $x_1, x_2, \ldots, x_n$, as shown in equation 2.21 is called multiple linear regression.

$$Y = \beta_0 + \beta_1 x_1 + \beta_2 x_2 + \ldots + \beta_n x_n \tag{2.21}$$

In this project, the REG procedure was used to predict the weight of sweetpotatoes.

The DISCRIM Procedure

The DISCRIM procedure computes various discriminant functions for classifying a set of observations in one or more groups based on one or more quantitative variables [21, 22]. For example, consider 3 groups as shown in Figure 2-5, where the Mahalanobis or Euclidean distance can be used to determine proximity.

The Mahalanobis distance is given by

$$d^2 = (\mathbf{x} - \mathbf{m}_\mathbf{x})' \mathbf{C}_\mathbf{x}^{-1} (\mathbf{x} - \mathbf{m}_\mathbf{x}) \tag{2.22}$$

where $\boldsymbol{x}$ is the feature vector with mean vector $\mathbf{m}_\mathbf{x}$ and covariance matrix $\mathbf{C}_\mathbf{x}$. In data sets where the features are uncorrelated and the variance is the same in all the direction, the covariance matrix is equal to the identity matrix and the distance is given by the square of the Euclidean distance. The Mahalanobis distance has advantages over the Euclidean distance in data sets, which contain different complex classes. It also performs significantly when the data sets are highly correlated. The DISCRIM procedure was used to grade the sweetpotatoes into various categories.

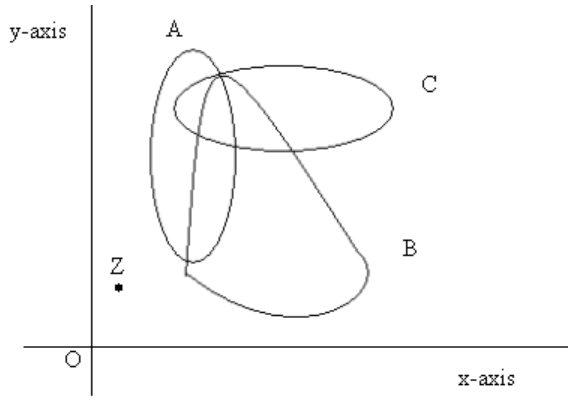

Figure 2-5: Distribution of datasets

Neural Networks

Neural networks have been the choice of researchers for years to perform classification apart from their applications in speech recognition, remote sensing, robotics, etc [23]. They perform with high speed and robustness over large data sets compared to conventional techniques. Neural networks process information similar to the human brain. A neural network consists of several interconnected neurons which operate in parallel to solve the specified problem with the help of the initial information provided during training. Figure 2-6 shows a neural network model that adjusts it weights according to the error that is propagated by comparing the neural network output, *y(n)* to the actual results, *y'(n)*.

Neural networks consist of layers of nodes connected by weighted links. The datasets are fed to the neural network through the input layer connected to the hidden layer where the actual processing is done and the output is calculated. Nodes in the network can be connected in different manners. Three popular network architectures are:

1) single-layer feed forward networks, in which the input layer is connected to the output layer, but not vice versa, 2) multilayer feed forward networks, similar to the single layer feed forward network but has one or more hidden layers and 3) recurrent network, in which the outputs of a layer can be feed to the previous layers in a feedback loop.

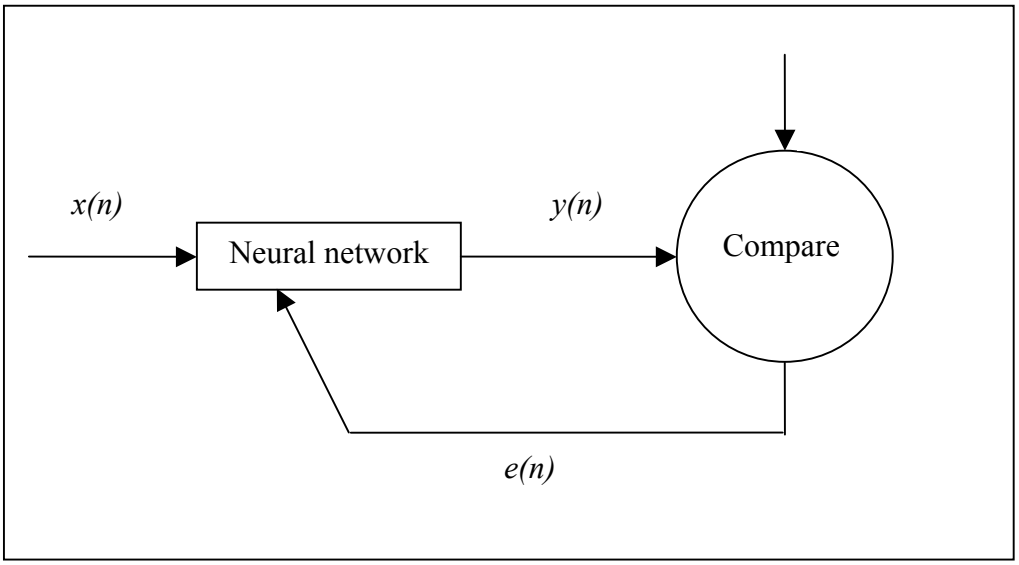

Figure 2-6: Neural network model

Once a network is structured it is ready to be trained. Weights are set randomly initial to start this process. Two approaches for training a network are supervised training and unsupervised training. In supervised training the desired output is feed to the network generally along with the inputs. In unsupervised training the network is trained with the help of the inputs only, no external information of the desired output is provided. A feed forward back propagation neural network makes an initial guess of the weight and starts training with the provided input data set. The error between the predicted and actual

value is propagated backwards to adjust the weight accordingly. All the neural networks in this study are built and trained with feed forward back propagation algorithm using Stuttgart Neural Network Simulator [24].

CHAPTER III

SYSTEM OVERVIEW

The aim of this chapter is to provide an overview of the instrument built for data acquisition. A basic diagram is shown in Figure 3-1. The main components of the data acquisition system are computer, camera, frame-grabber, global positioning system receiver, lighting, and a wooden enclosure. Section 3.1 discusses the physical components of the data acquisition system. The data collection procedure is given in section 3.2.

3.1 Data Acquisition

The data acquisition system must satisfy few specifications, which can be summarized as follows.

- The instrument should be able to perform over a large span of time without any interruptions.
- The instrument should be able to perform in harsh environmental conditions, e.g. dusty environment, temperature range from $-10^0 C$ to $45^0 C$, and shock.
- The instrument should consume low power.
- The instrument should perform with high efficiency.

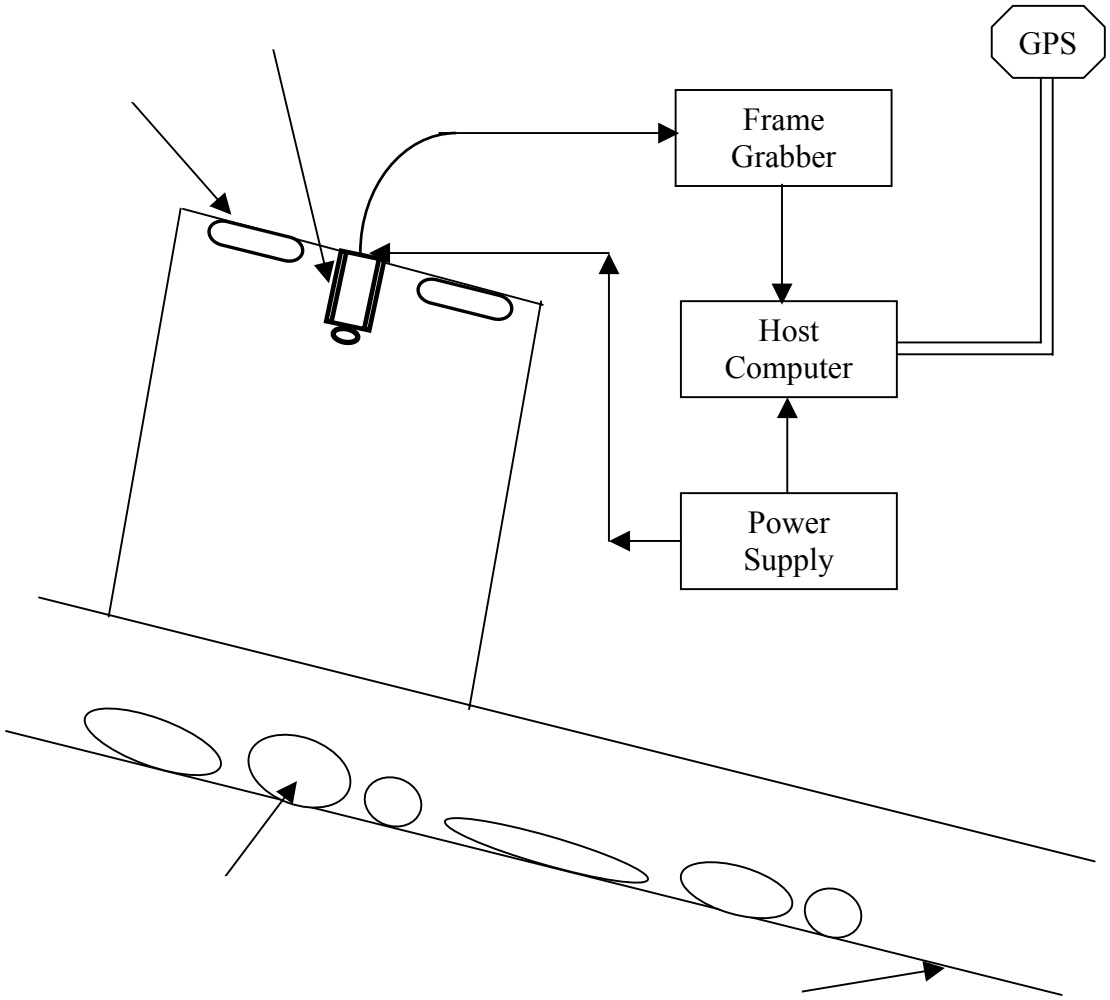

Figure 3-1: Hardware overview

Wooden Enclosure

An enclosure is used to block the light from outside. It is constructed with angle iron edges and plywood sides with a size of 36*24*36 inches. A six-inch opening at the bottom along the width is made to allow sweetpotatoes to pass under the edge of the enclosure. The inside of the enclosure is painted black. A black metal sheet is fixed below the conveyor belt where the enclosure is mounted to block reflected sunlight. The gaps at the bottom of the enclosure are covered with hanging canvas, which blocks light but still allows sweetpotatoes to pass through. The height of the enclosure is designed according to the focal length of the camera lens.

Conveyor Belt

Sweetpotatoes harvested with the digger are transported to the sorting area with a conveyor belt. The speed of the conveyor belt is an important factor to be taken into consideration. The high speed of the conveyor belt results in blurring of the images. The image data acquisition speed should be increased proportionately with an increase in the speed of the conveyor belt to ensure coverage of the entire field.

Camera

Images are captured with a Pulnix TMC-9700 digital camera. It is a three-chip CCD color high-resolution, progressive scan camera with asynchronous reset capability, adjustable shutter speed, and continuous video output. The camera works with a 12V DC power supply and can withstand temperatures ranging from -10^0C to 50^0C. Some of the important features of the camera are lens, shutter speed, and aperture.

- **Lens:** It is important to select the appropriate lens that would allow coverage of the entire width of the conveyor belt. The height of the wooden enclosure is determined from the focal length of the camera lens. A Fujinon HF9A-2MI lens is used.

- **Shutter Speed:** The camera shutter speed must be high enough to reduce blur images. The shutter rate is adjustable from 1/60 to 1/16,000. An increase in the shutter speed decreases the amount of light for proper exposure. A shutter rate of 1/125 sec is selected to be ideal for the system with the available lighting.
- **Aperture:** To compensate for the increase in the shutter speed, the aperture of the lens is adjusted to allow enough light for proper exposure.

Frame-grabber

The frame grabber is used to capture images from a continuous video signal and store them in the computer memory. An Integral Flashbus MVPRO frame grabber is used to grab images. One of the important features of the frame grabber is the "align" feature, which sets the parameter for the first video field to be captured when a video capture is triggered. Three types of align are available, *even*, *odd,* and *any*. *Even* captures an *even/odd* frame. *Odd* captures an *odd/even* video frame, and *any* captures the next video frame. Improper setup of the align results in blurred images. *Even* align is used for this project.

The frame grabber can be programmed using media control interface (MCI) commands to automatically set the frame grabber to capture and store images in

sequential order at a desired delay [25]. A file is also created to store the information about the time the image is captured. This is for later use to relate the images with the GPS information to produce yield maps. This will be discussed later in chapter IV.

Global Positioning System

A global positioning system (GPS) was originally designed by the U.S. Department of Defense as a satellite-based navigation system, but it is currently used for many other purposes including precision agriculture. The GPS provides specially coded signals from satellites, which can be processed by a GPS receiver to compute position, velocity, time, and various other details. The nominal GPS Operational Constellation consists of 24 satellites that orbit the earth in 12 hours. A minimum of 4 satellites is required to compute the position and other information. The port setting for the GPS was set to 4800-8-0-1, where 4800 is the baud rate, 8 is the number of data bits, 0 is the parity bit, and 1 is the stop bit. The baud rate specifies the speed at which the GPS receiver transmits. Within the GPS receiver the received data bits are aligned and checked for errors with the parity bit.

The position information of the system is required to produce yield maps, which shall be discussed later in this thesis. A Trimble AgGPS 132 is used, which runs on a 12V DC power supply from the tractor.

Lighting

Lighting is an important factor for the system to operate in all conditions, irrespective of varying ambient light intensity. Lights are mounted in the top of the

enclosure along with the camera. Six 55-W quartz halogen lights are fixed to provide uniform illumination.

3.2 Design Considerations

For the generation of a yield map, it is important to obtain image information of the entire field. Thus images were captured at a delay of 1 second and the speed of the conveyor belt is set to 1 mile/hour. For 1 second, the conveyor would move a distance of 36 inches. The distance is equal to the length of the enclosure (the camera's field of view).

The system is designed to consume low power. The entire system is operated on a 12V DC power supply from the tractor. A separate box was constructed for the industrial computer to protect it from dust during harvest. Figure 3-2 shows the setup on the tractor.

Figure 3-2: Experimental setup

Many factors are taken into consideration in detecting and grading of sweetpotatoes. Figure 3-3 shows some of the example images that cause difficulties in detection and grading of sweetpotatoes. The issues to be considered to ensure good results can be summarized as follows:

- The speed of the conveyor belt should be moderate for the frame grabber to grab images at regular intervals. An increase in the speed causes blur red images. The usage of a high-speed digital camera with continuous video streams would be ideal.
- The lighting provided for the system should be fairly high in order to obtain images with good quality. The lighting should provide uniform illumination.
- Care should also be taken so that the lighting conditions do not affect the performance of the system.
- The material coming up on the conveyor belt should be distributed evenly to make segmentation possible and reduce the error rate.
- The soil should not be damp causing mud to cling to the sweetpotatoes, thus making them hard to detect. Harvest should be carried out only when the soil is relatively dry.

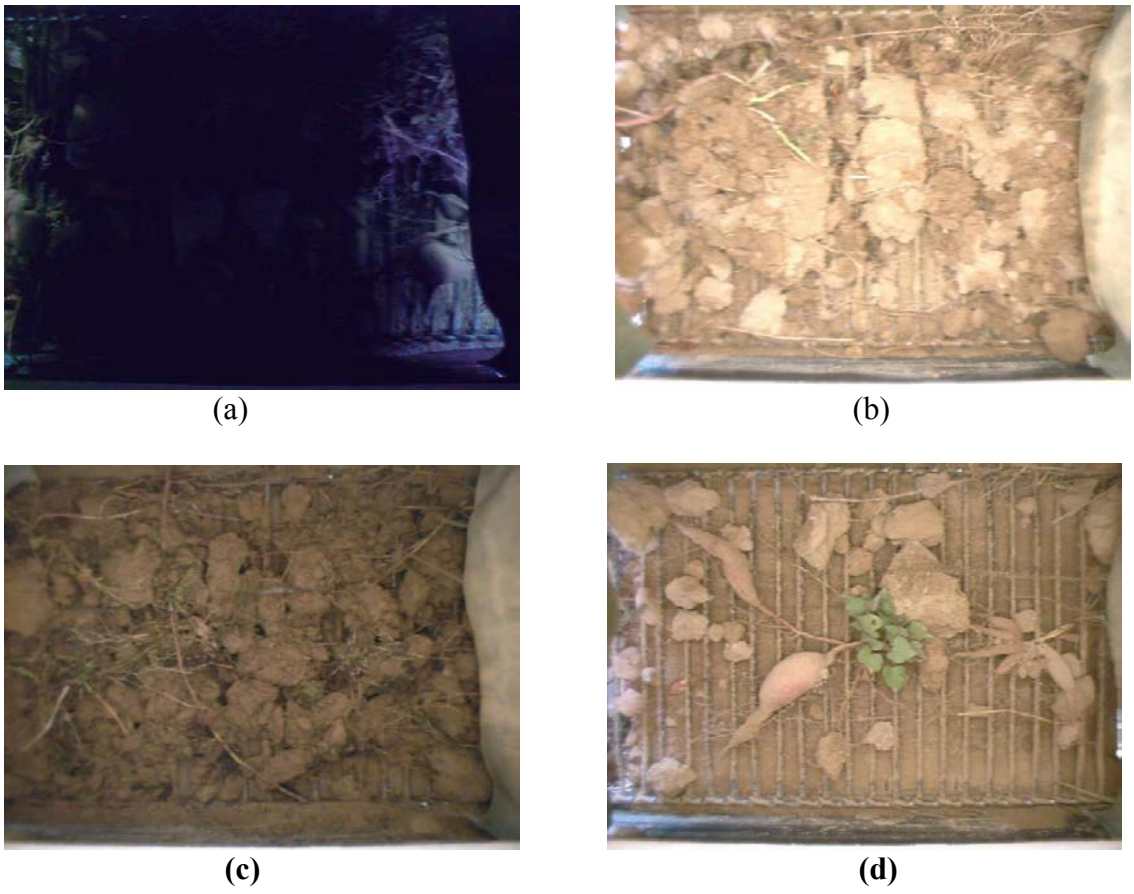

(a) (b)

(c) **(d)**

Figure 3-3: Illustrative examples depicting the difficulty in detection of sweetpotatoes. (a) Insufficient lighting and uneven illumination, (b) Heavy load, (c) Wet soil covering the sweetpotatoes, and (d) Good image.

CHAPTER IV

EXPERIMENTAL DETAILS

Experiments were conducted over a 1.5 acre field at the MAFES/Pontotoc Experiment Station, Mississippi. Initially, the wooden box enclosure mounted on the conveyor belt ahead of the sorting area. The camera that was connected to the industrial computer was mounted in the top of the box. The GPS antenna was placed atop the harvester as shown in Figure-3.3. The spatial information from the global positioning system was used to geo-reference the images to create yield maps. During harvest, the sweetpotatoes along with the soil are carried to the sorting area on the conveyor belt. Images of the scene on the conveyor belt were captured with the frame grabber and stored on the hard drive of the computer. Approximately 20,000 images were collected for later analysis. In the 1.5 acres, 37 plots of 10 feet long were marked. Sweetpotatoes that were harvested from the 10 feet plots were labeled and stored in different containers and manually graded later on. Images were collected during the harvest along with the GPS information, and were later processed in the laboratory. For the purpose of grading the sweetpotatoes and estimating the weight, 15 culls, 15 canners, 13 U.S. No. 1, and 12 jumbos were brought to the laboratory and were labeled as graded dataset. Images of these sweetpotatoes were used to develop a relationship between image-based size and shape and the grade and weight of sweetpotatoes. The data from the 10 feet plots was

labeled as un-graded data. The performance of the algorithms was tested on the un-graded dataset. The information required for yield monitoring is summarized below. Figure 4-1 shows same images taken during the harvest.

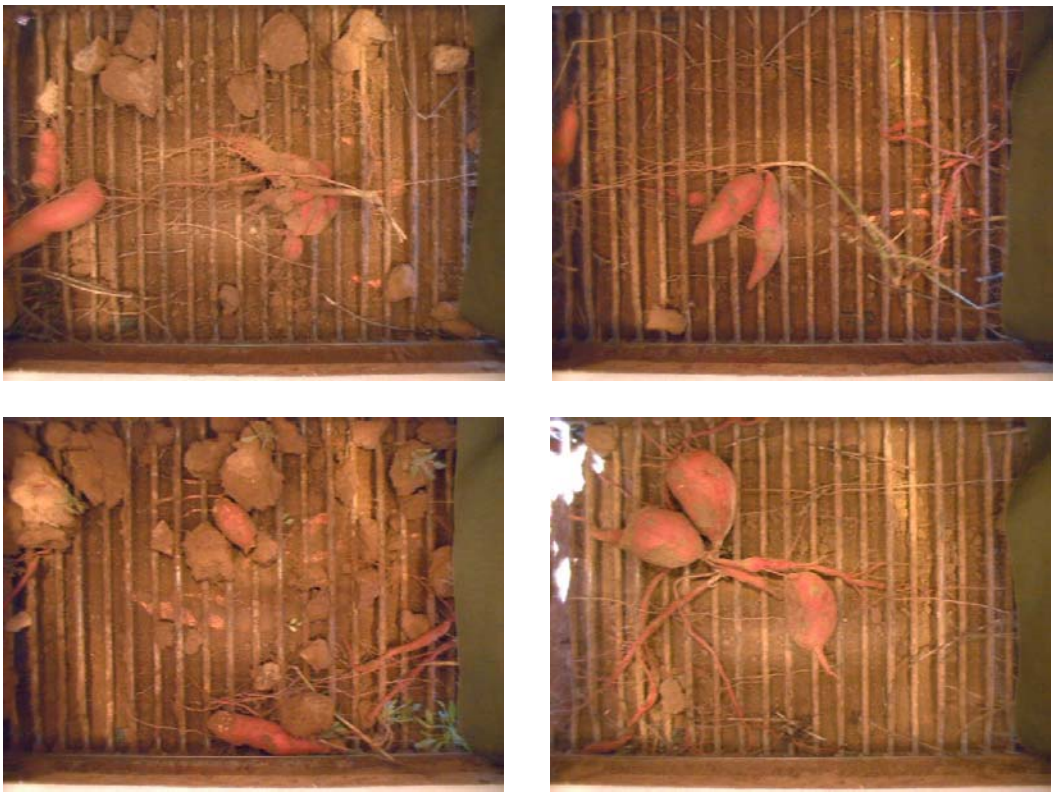

Figure 4-1: Sample images taken during harvest of sweetpotatoes at the MAFES/Pontotoc Experiment Station.

4.1 GPS Information

A GPS receiver was mounted on the harvester and connected to the computer through the serial port. The configuration of the GPS receiver was set to 4800-8-0-1. The output of the GPS receiver consists of four different strings of information GPVTG, GPGSA, GPRMC, and GPGGA. Figure 4-2 shows a sample of the GPS receiver output.

The GPRMC string was used to extract the latitude and longitude information. The 4th and the 6th string of the GPRMC string correspond to the latitude and the longitude respectively.

```
$GPVTG,0.0,T,,,000.00,N,000.00,K,D*45
$GPGSA,A,3,09,14,15,17,18,21,23,29,,,,,2.8,1.1,2.5*31
$GPRMC,141515,A,3408.323626,N,08900.535608,W,000.00,0.0,091001,0.8,E,D*3B
$GPGGA,141516.00,3408.323624,N,08900.535608,W,2,08,1.1,142.86,M,29.07,M,2.6,0160*7
$GPVTG,0.0,T,,,000.00,N,000.00,K,D*45
$GPGSA,A,3,09,14,15,17,18,21,23,29,,,,,2.8,1.1,2.5*31
$GPRMC,141516,A,3408.323624,N,08900.535608,W,000.00,0.0,091001,0.8,E,D*3A
```

Figure 4-2: GPS receiver data

The GPS receiver data was stored in files for later use to geo-reference the images for yield and grade maps. The data file contained information of the time of arrival of every string of the GPS data. This information was stored in a text file as shown in Figure 4-3.

```
Time                        GPS data
9:25:13 $GPVTG,0.0,T,,,000.00,N,000.00,K,D*45
9:25:14 $GPGSA,A,3,09,14,15,17,18,21,23,29,,,,,2.8,1.1,2.5*31
9:25:14 $GPRMC,141515,A,3408.323626,N,08900.535608,W,000.00,0.
9:25:14 $GPGGA,141516.00,3408.323624,N,08900.535608,W,2,08,1.1
9:25:14 $GPVTG,0.0,T,,,000.00,N,000.00,K,D*45
9:25:15 $GPGSA,A,3,09,14,15,17,18,21,23,29,,,,,2.8,1.1,2.5*31
9:25:15 $GPRMC,141516,A,3408.323624,N,08900.535608,W,000.00,0.
9:25:15 $GPGGA,141517.00,3408.323623,N,08900.535608,W,2,08,1.1
9:25:15 $GPVTG,0.0,T,,,000.00,N,000.00,K,D*45
9:25:16 $GPGSA,A,3,09,14,15,17,18,21,23,29,,,,,2.8,1.1,2.5*31
9:25:16 $GPRMC,141517,A,3408.323623,N,08900.535608,W,000.00,0.
9:25:16 $GPGGA,141518.00,3408.323621,N,08900.535607,W,2,08,1.1
9:25:16 $GPVTG,0.0,T,,,000.00,N,000.00,K,D*45
9:25:17 $GPGSA,A,3,09,14,15,17,18,21,23,29,,,,,2.8,1.1,2.5*31
```

Figure 4-3: GPS data file format

4.2 Image Collection

Along with the GPS receiver data, images of the sweetpotatoes during harvest are also required to analyze the yield. These images were captured with a frame grabber inserted into the PCI slot of the industrial computer. A camera was attached to the frame grabber, and it outputs continuous video streams. The shutter rate of the camera was set to 1/125 sec. A program was written in Microsoft Visual C++ with media control interface (MCI) commands to capture images with the frame grabber and store the images in memory. Images were collected with a delay of 1 second and saved as JPEG's. Figure 4-4 shows the outline of this process.

A time stamp is necessary to correlate the images to a particular location. A text file was created to save the time information. The time stamp was written to the file along with the filename for every image file saved. The procedure for extracting the information from these files and generating yield maps shall be discussed later in chapter V.

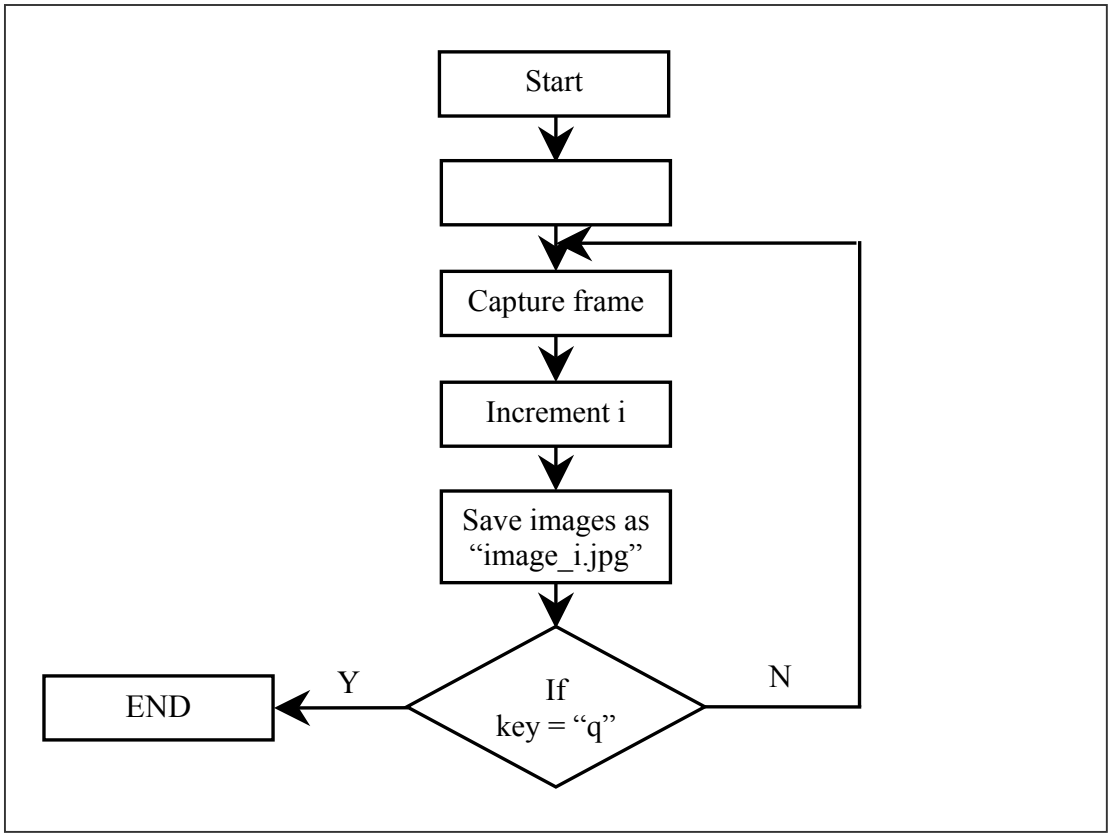

Figure 4-4: Flow chart of the image storage program

CHAPTER V

SOFTWARE APPROACH

Having discussed the hardware setup and the theoretical background for various image processing techniques, this chapter presents the software approach used in identifying and grading sweetpotatoes. The software is developed for the detection and grading of sweetpotatoes with Borland C++ Builder version 5.0 [26]. A graphical user interface is created to open images and perform image processing algorithms to detect and grade the sweetpotatoes. The GUI also enables the user to visualize the intermediate stages in the detection and grading processes. Figure 5-1 shows the GUI developed for the user interface. The images are divided into two regions: Foreground and background. The foreground pixels correspond to the sweetpotatoes. Section 5.1 describes the techniques used for the identification of the location of the sweetpotatoes. Section 5.2 discusses retrieving the shape of the located objects. Section 5.3 explains the various features that are used to grade the sweetpotatoes.

Figure 5-1: GUI developed for the grading and detecting of sweetpotatoes.

5.1 Identification of Object Location

Before detecting the sweetpotatoes, the foremost task would be to identify the location of the sweetpotatoes. A simple approach of object identification is by thresholding. But the RGB values of the pixels corresponding to the sweetpotatoes do not vary much from the RGB values of the mud. Therefore a proper threshold value cannot be derived.

An alternative approach is to use the YUV color model which is widely used by PAL, NTSC, and SECAM composite color video standards [27]. Y represents the luminance. U and V represent the chrominance. The chrominance can be defined as the difference between a color and a reference white at the same luminance. Conversion of RGB values into the YUV color model is shown in equation 5.1.

$$\begin{pmatrix} Y \\ U \\ V \end{pmatrix} = \begin{pmatrix} 0.299 & 0.587 & 0.114 \\ -0.147 & -0.289 & 0.436 \\ 0.615 & -0.515 & -0.100 \end{pmatrix} \begin{pmatrix} R \\ G \\ B \end{pmatrix} \tag{5.1}$$

or,

$$Y = 0.299R + 0.587G + 0.11B \tag{5.2}$$

$$U = (B - Y) * 0.493 \tag{5.3}$$

$$V = (R - Y) * 0.877 \tag{5.4}$$

From equation 5.4, the color difference component V is used to highlight the red in the image, taking advantage of the sweetpotato's color which lies between pink and orange. Figure 5.2 shows sample histograms for the color difference component V for two images with and without sweetpotatoes. From the sample histograms shown below and from various other histograms of other images, it is concluded that a V value greater than 65 is observed only in images that contain sweetpotatoes, irrespective of the presence of mud. This value is used as a threshold to identify the location of the sweetpotatoes. Figure 5-3 shows the threshold image of the sample image shown in Figure 2-2.

From Figure 5.3, it can be concluded that the white pixels in the image correspond to the location of the sweetpotatoes. Identifying the location of the sweetpotatoes decreases the search space for locating the sweetpotatoes, which is directly proportional to the decrease in the number of computations. A region growing algorithm is developed for retrieving the complete shape of the sweetpotatoes, which will be discussed in the following section.

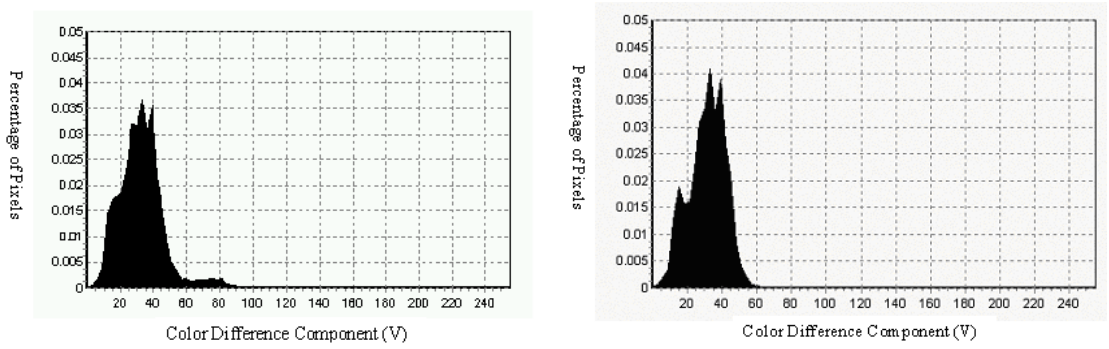

(a) (b)

Figure 5-2: Sample histograms of sweetpotato harvest images. (a) A typical plot of an image, with sweetpotatoes. (b) A typical plot of an image without sweetpotatoes.

Having identified the location of the sweetpotatoes and the boundaries, it is necessary to ensure that the pixels corresponding to the sweetpotatoes be highlighted. Few characteristics of real sweetpotatoes that help in the segmentation can be summarized as follows:

- The sweetpotatoes will have a continuous boundary.
- They have a connected surface without the presence of any holes on the surface.

Using the above characteristics, the sweetpotatoes pixels can be differentiated from the background.

Figure 5-3: Thresholding with respective to the V component at a value of 65.

5.2 Region Growing

Image segmentation is an approach of grouping all the pixels in an image together into regions of similarity [28, 29]. There are two main approaches to segmentation: region splitting and region growing. Region splitting is a divide and conquer procedure, which splits the area of interest into 4 equal sub-areas. The pixels in a sub-area are analyzed on the basis of some constraints to decide if they belong to a region. If not, this sub-area is further divided into 4 equal sub-areas and the procedure is repeated until no future splitting occurs.

Region growing, on the other hand, is the opposite of region splitting. An initial seed pixel is selected in the image or region of interest. All the neighboring pixels of the seed pixel are analyzed on the basis of some constraints. Neighboring pixels that are similar to the seed pixel are added to the seed pixel region, increasing the size of the region. This process is repeated for all the added pixels until the region stops growing. The whole process is continued until all the pixels of the image are categorized into some region. For example Figure 5-4 shows the process of region growing. The black pixels

indicate the boundary of an object. Region is grown with respect to the seed pixel till the boundary is encountered.

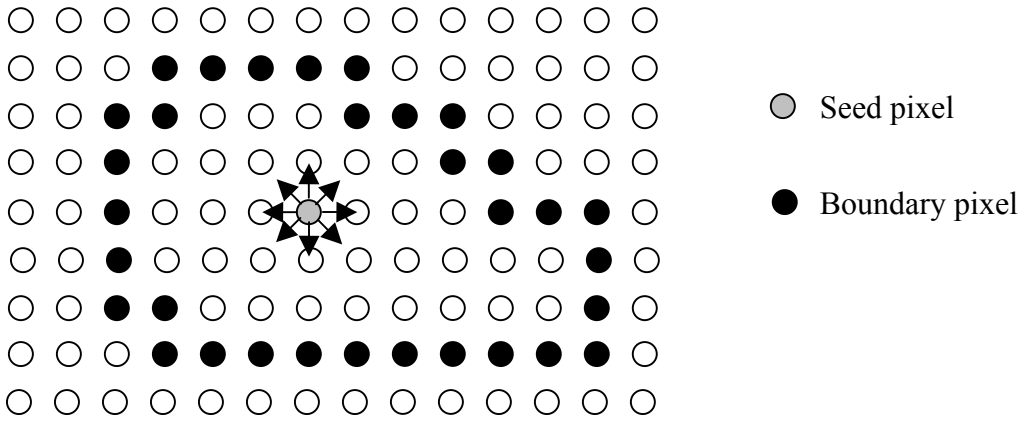

Figure 5-4: Region growing algorithm

Utilizing the information of the object location obtained in section 5.1, the region growing algorithm is performed. The region is grown with respect to the pixels with a threshold greater than 65 for the V component. If the neighboring pixels are identified as belonging to the sweetpotatoes, the pixels are added to the region growing. A neighboring pixel is considered to correspond to a sweetpotato if it does not belong to an edge pixel. Also the textural information of the pixel is used. In brief, the region is grown with the information of the texture until an edge is encountered. The region growing algorithm performed on the test image is shown in Figure 5-5.

It is noteworthy to mention that a filter is used to remove all the objects that are too small after performing a threshold on the V component of the image. This process of filtering enables unwanted roots, that are detected with the algorithm, to be removed. Additional detected roots also can be removed with the help of statistical analysis, which

will be discussed later in this chapter. Figure 5-6 shows the flow chart for the sweetpotato detection algorithm.

Figure 5-5: Region growing algorithm performed on the test image

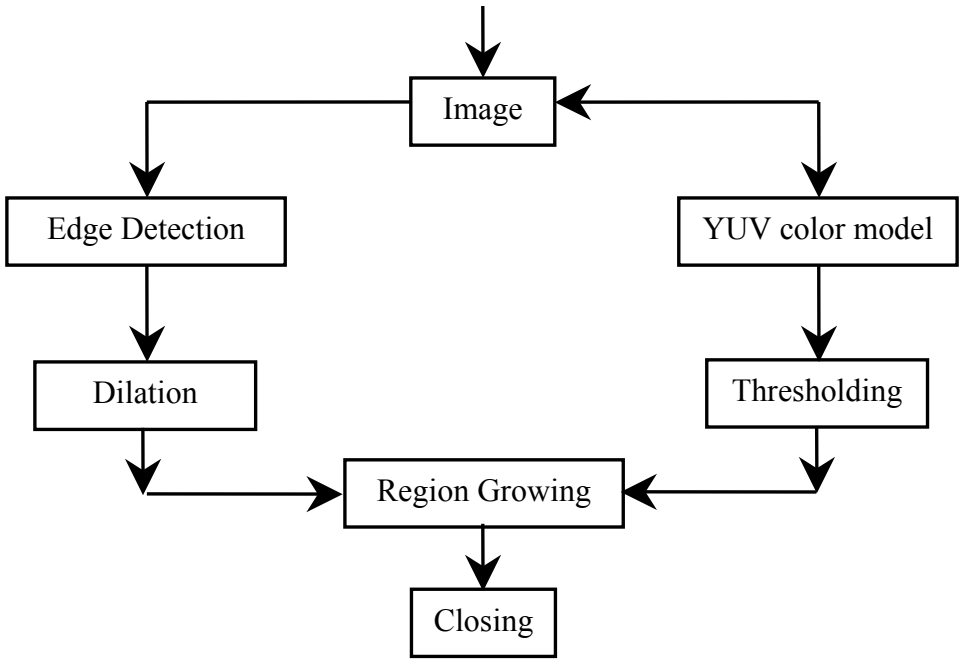

Figure 5-6: Flow chart of sweetpotato detection algorithm

5.3 Feature Extraction

For the estimation of the weight and grade of the sweetpotatoes, various features are extracted from the images, which are processed to highlight the pixels belonging to the sweetpotatoes. As discussed in section 2.3, the polar moment of inertia assists in analyzing the shape of the object. The polar moment of inertia of each sweetpotato detected is calculated along with its area. Each pixel is considered to be a unit in these measurements. The width and height of a rectangle, which can be drawn around the detected sweetpotatoes, are also extracted. Finally, considering that the shape of sweetpotatoes is elliptical, the lengths of the major and minor axes are also extracted. These features are used to build different classifiers that will be discussed in section 6.1.

5.4 Yield Maps

The objective of this study consists of three stages: building of an image acquisition system, develop algorithms for segmentation and estimating the weight and grade, and generating yield maps.

Having discussed the techniques used for image segmentation and weight and grade estimation, this section discusses how this information can be summarized to produce yield maps. The results obtained from the weight and grade estimation are used along with the spatial information from the global positioning system to geo-reference the images. Figure 5-7 shows the flow chart for the generation of yield and grade maps. Three types of input are required for this: A GPS data file as shown in Figure 4-3, an image data file as mentioned in Section 4.2, and the collected JPEG images.

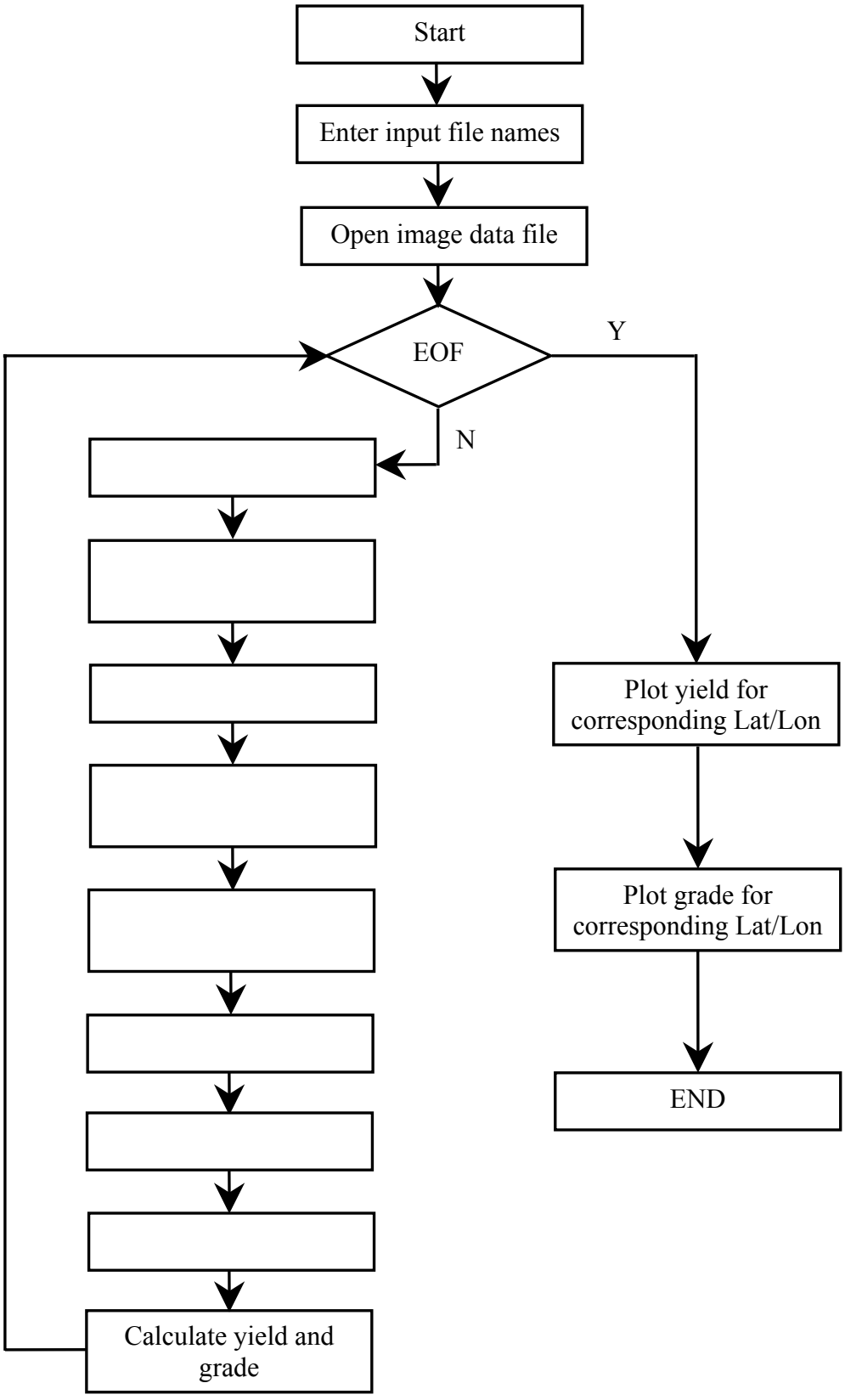

Figure 5-7: Flow chart for generating yield maps from GPS and image data

On the other hand, more than one image can correspond to one latitude and longitude. In this scenario, the information from all the images are summed up and geo-referenced to that specific location. Figure 5-8 shows the flow chart for the yield estimation. ESRI Arc View software is used to generate yield maps.

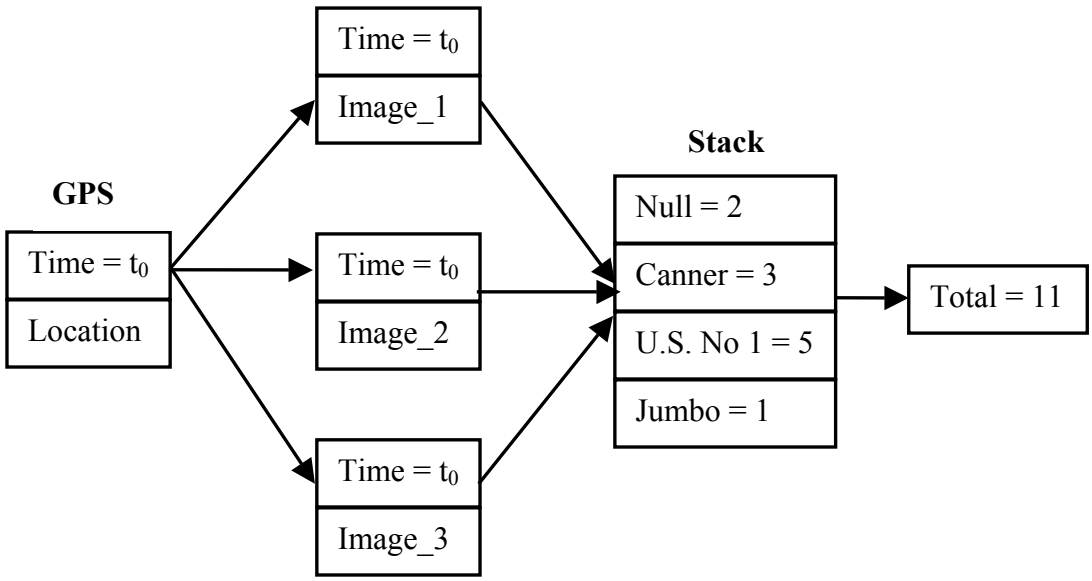

Figure 5-8: Flow chart for the estimation of yield for a given latitude and longitude

CHAPTER VI

RESULTS

A data acquisition system is developed for yield monitoring of sweetpotatoes. Data is collected over a 1.5-acre field at the MAFES/Pontotoc Experiment Station, Mississippi. Image segmentation algorithms are used to detect the sweetpotatoes. The algorithms performed with an accuracy of 80% in identifying the sweetpotatoes on the un-graded data. It is observed that the system could not detect sweetpotatoes located along the boundaries of the images due to poor lighting, and also in cases where sweetpotatoes are covered with mud. For example, Figure 6-1 and 6-2, respectively, show the output images from the image segmentation algorithm due to poor lighting and sweetpotatoes covered with mud. The algorithm also did not perform well in separating sweetpotatoes that are located too close to each other. Figure 6-3 shows an example illustrating this problem.

To estimate the weight and grade of the sweetpotatoes from the images, two types of data sets; graded and un-graded, are used as discussed in Chapter IV. Statistical methods and neural networks are used for the estimation.

(a)

(b)

Figure 6-1: (a) Image with sweetpotato located at the boundary of the image. (b) Illustration of the failure of the image segmentation algorithm in case of poor lighting.

(a)

(b)

Figure 6-2: (a) Image with sweetpotatoes covered with mud. (b) Illustration of the failure of the image segmentation algorithm on sweetpotatoes covered with mud.

(a) (b)

Figure 6-3: (a) Image with sweetpotatoes located too close to each other. (b) Illustration of the failure of the image segmentation algorithm on such sweetpotatoes.

6.1 Classifiers

Wooten et al. studied the correlation of image based size of sweetpotatoes and the polar moment of inertia to the grade and weight the sweetpotatoes [6]. In this study, image based size, polar moment of inertia, width, length, and the length of the major and minor axes are considered with respect to the grade and weight. Accordingly, four classifiers that use different inputs for prediction have been developed. Classifier 1 uses only pixel area and polar moment of inertia to perform weight and grade prediction. Classifier 2 uses width and height of sweetpotatoes along with pixel area and polar moment of inertia to predict the weight and grade. Classifier 3 uses length of the major and minor axes of sweetpotatoes along with pixel area and polar moment of inertia. Classifier 3 is important because of the varying orientation of sweetpotatoes on the conveyor belt when the images are captured. It also enables us to distinguish long thin

roots, which are generally misclassified. Classifier 4 uses all the available information: pixel area, polar moment of inertia, width, height, and length of the major and minor axes of the sweetpotatoes to predict the weight and grade.

6.2 Preparation of Training and Test Datasets

Features that are extracted from the images are used to perform the weight and grade analysis with statistical methods and neural networks. For statistical methods, the features are not preprocessed but are fed directly. For neural networks, on the other-hand, it is important to preprocess the features extracted. Features are normalized between –1 and 1. Stuttgart Neural Networks Simulator is used to build the networks.

6.3 Evaluation of Graded Data

For the purpose of developing a relation between the image based size and shape and the weight and grade of sweetpotatoes, graded sweetpotatoes are collected for experimental purpose. This data set of graded sweetpotatoes consists of 15 culls, 15 canners, 13 U.S. No. 1, and 12 jumbos. Images of these sweetpotatoes are processed, and associated features are extracted. Apart from these features, features are also extracted from associated images in which pixels corresponding to the sweetpotatoes are manually "painted" white. For simplicity of explaining the problem, the two feature sets are called painted and detected.

This procedure of comparing the results of the painted and detected datasets will estimate the error of the system due to the detection of the sweetpotatoes in the image. The weight and grade analysis that is performed on these sets follows.

Weight Estimate

The two feature sets from the painted and detected sweetpotato images are analyzed using statistical methods and neural networks. Figure 6-4 shows the results of the performance of the 4 classifiers on the data set with the REG procedure. It is observed that REG procedure performed better on the painted sweetpotato images than detected sweetpotato images. Classifier4 produced the highest accuracy for both painted and detected sweetpotato images. An accuracy rate of 0.9756 and 0.9583 respectively are obtained with classifier4 using statistical methods. Figure 6-5 shows the results obtained from using a feed forward back propagation neural network with 10 hidden nodes and 1 output node. Results similar to the results obtained using statistical methods are observed. An accuracy rate of 0.9463 and 0.9336 respectively are obtained with classifier4 using neural networks. It can be concluded that image based size and shape can be used to estimate the weight of the sweetpotatoes.

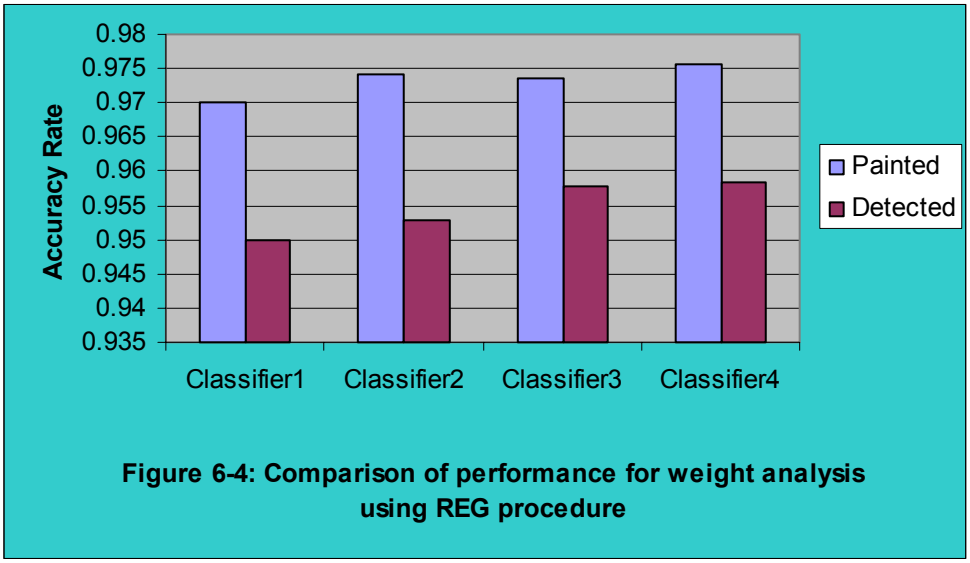

Figure 6-4: Comparison of performance for weight analysis using REG procedure

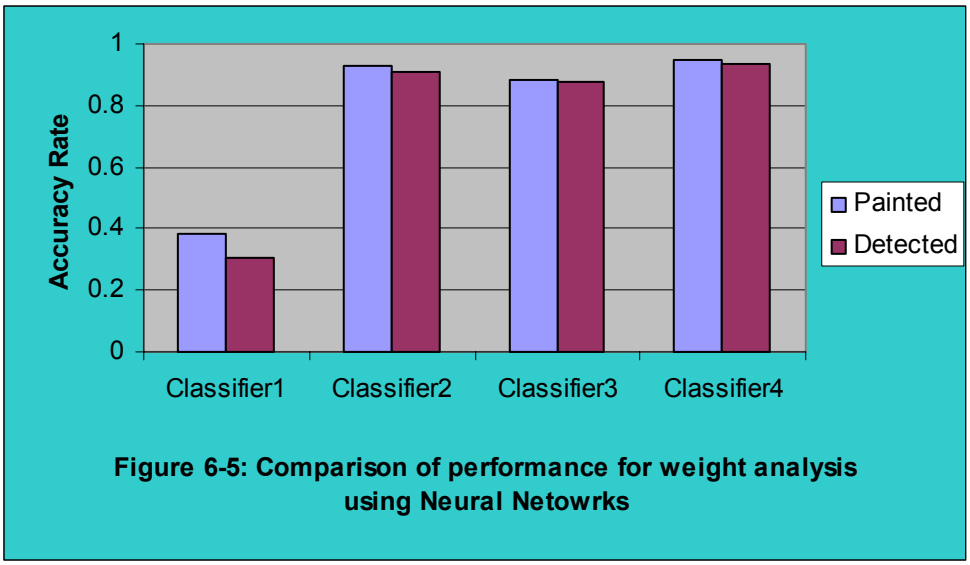

Figure 6-5: Comparison of performance for weight analysis using Neural Netowrks

Grade Estimate

A procedure similar to that of the weight estimate is used for grading sweetpotatoes into nulls, canners, U.S. No. 1's, and jumbos. The DISCRIM procedure is used instead of the REG procedure. Features are extracted from the painted and detected images and graded using four classifiers as mentioned in section 6.1. Classifier4 outperformed the other classifiers using statistical methods and neural networks. Figure 6-6 shows the performance of grade estimation using classifier4 with the DISCRIM procedure on the painted and detected sweetpotato image features. Canners, U.S. No.1's and jumbos are predicted with 100% accuracy for painted sweetpotato images. The accuracy for detected sweetpotato images decreased slightly compared to painted sweetpotato images. It is observed that culls have the highest error rate compared to the other grades of sweetpotatoes. An accuracy of 73.33% for painted sweetpotato images and an accuracy of 66.67% on detected sweetpotato images are obtained for culls. Figure

6-7 shows the performance of grade estimation using classifier4 with neural networks on the different feature sets. Canners, U.S. No.1's and jumbos have the highest accuracy rate. An accuracy of 80% for painted sweetpotato images and an accuracy of 73.33% on detected sweetpotato images are obtained for culls. The error in culls can be attributed to their varying size and shape. The performances of all the classifiers are listed in Table 6-1 and Table 6-2.

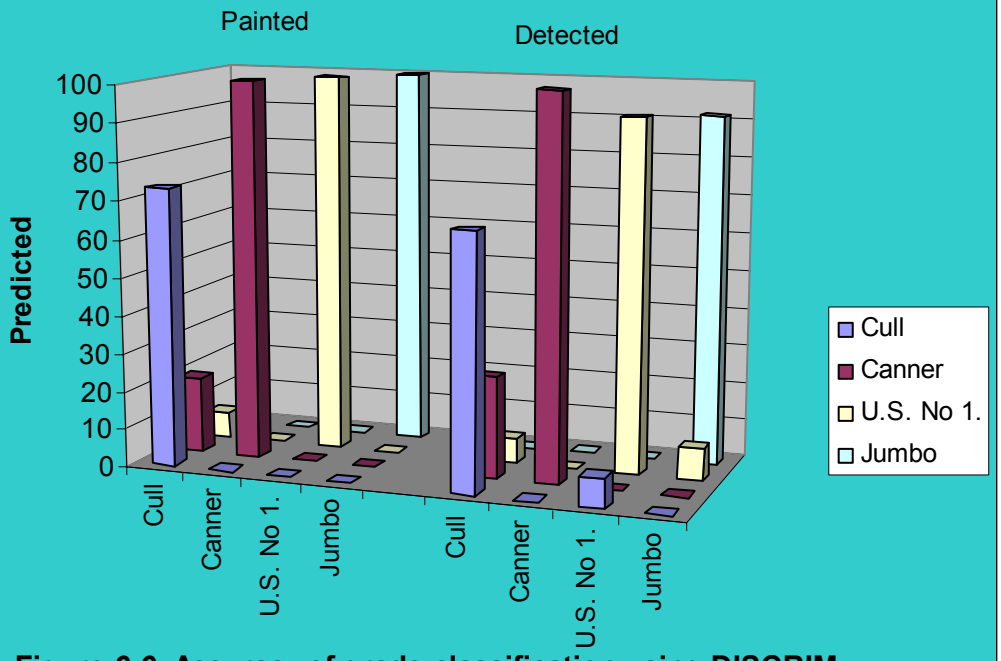

Figure 6-6: Accuracy of grade classification using DISCRIM procedure

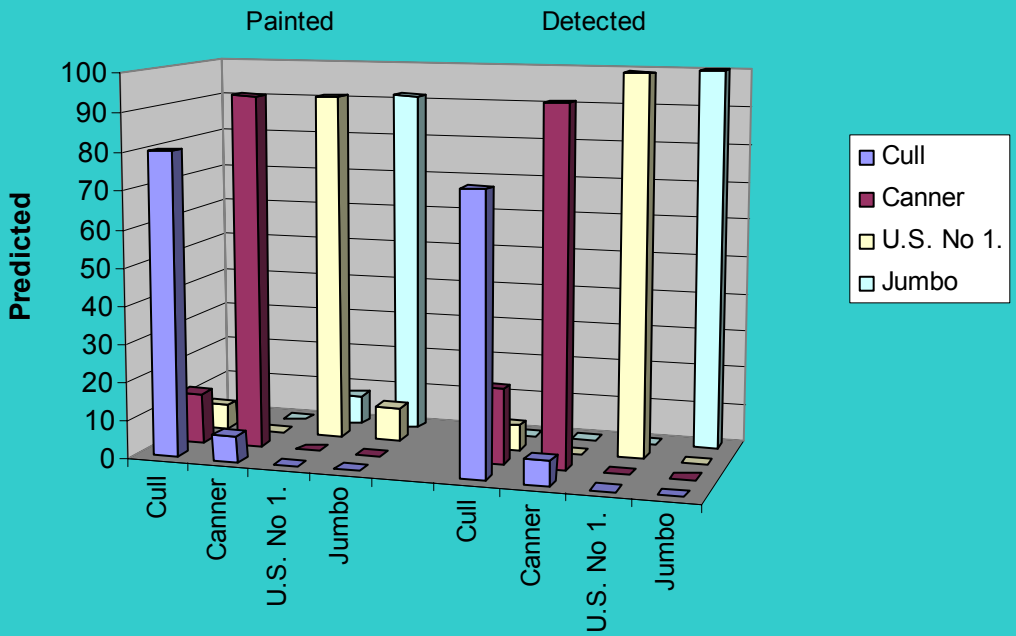

Figure 6-7: Accuracy of grade classification using Neural Networks

Table 6-1: Accuracy of grade classification for different classifiers using DISCRIM procedure.

Actual\Predicted		Painted				Detected			
		Cull	**Canner**	**U.S. No 1.**	**Jumbo**	**Cull**	**Canner**	**U.S. No 1.**	**Jumbo**
Classifier1	**Cull**	46.67	46.67	6.67	0.00	33.33	40.00	26.67	0.00
	Canner	0.00	100.00	0.00	0.00	6.67	93.33	0.00	0.00
	U.S. No 1.	0.00	7.69	92.31	0.00	0.00	0.00	100.00	0.00
	Jumbo	0.00	0.00	0.00	100.00	0.00	0.00	8.33	91.67
Classifier2	**Cull**	60.00	33.33	6.67	0.00	53.33	26.67	20.00	0.00
	Canner	0.00	100.00	0.00	0.00	0.00	100.00	0.00	0.00
	U.S. No 1.	0.00	7.69	92.31	0.00	0.00	0.00	92.31	7.69
	Jumbo	0.00	0.00	0.00	100.00	0.00	0.00	8.33	91.67
Classifier3	**Cull**	60.00	33.33	6.67	0.00	60.00	26.67	13.33	0.00
	Canner	6.67	93.33	0.00	0.00	6.67	93.33	0.00	0.00
	U.S. No 1.	0.00	0.00	100.00	0.00	15.38	0.00	84.62	0.00
	Jumbo	0.00	0.00	0.00	100.00	0.00	0.00	8.33	91.67
Classifier4	**Cull**	73.33	20.00	6.67	0.00	66.67	26.67	6.67	0.00
	Canner	0.00	100.00	0.00	0.00	0.00	100.00	0.00	0.00
	U.S. No 1.	0.00	0.00	100.00	0.00	7.69	0.00	92.31	0.00
	Jumbo	0.00	0.00	0.00	100.00	0.00	0.00	8.33	91.67

Table 6-2: Accuracy of grade classification for different classifiers using Neural Networks.

Actual\Predicted		Painted				Detected			
		Cull	**Canner**	**U.S. No 1.**	**Jumbo**	**Cull**	**Canner**	**U.S. No 1.**	**Jumbo**
Classifier1	**Cull**	66.67	20.00	0.00	13.33	66.67	20.00	6.67	6.67
	Canner	26.66	46.67	0.00	26.67	20.00	53.33	13.33	13.33
	U.S. No 1.	0.00	15.38	15.38	69.23	0.00	23.08	38.46	38.46
	Jumbo	0.00	0.00	0.00	100.00	0.00	8.33	25.00	66.67
Classifier2	**Cull**	73.33	20.00	6.67	0.00	73.33	20.00	6.67	0.00
	Canner	13.33	86.67	0.00	0.00	6.67	93.33	0.00	0.00
	U.S. No 1.	7.69	0.00	69.23	23.08	15.38	0.00	76.92	7.69
	Jumbo	0.00	0.00	8.33	91.67	0.00	0.00	8.33	91.67
Classifier3	**Cull**	80.00	13.33	6.67	0.00	80.00	13.33	6.67	0.00
	Canner	13.33	86.67	0.00	0.00	6.67	93.33	0.00	0.00
	U.S. No 1.	7.69	7.69	46.15	38.46	23.08	0.00	53.84	23.08
	Jumbo	0.00	0.00	0.00	100.00	0.00	0.00	0.00	100.00
Classifier4	**Cull**	80.00	13.33	6.67	0.00	73.33	20.00	6.67	0.00
	Canner	6.67	93.33	0.00	0.00	6.67	93.33	0.00	0.00
	U.S. No 1.	0.00	0.00	92.31	7.69	0.00	0.00	100.00	0.00
	Jumbo	0.00	0.00	8.33	91.67	0.00	0.00	0.00	100.00

6.4 Evaluation of Un-graded Data

The evaluation experiments are carried out on the un-graded data collected at the MAFES/Pontotoc Experiment Station, Mississippi, as mentioned in Chapter IV. A total of 37 plots, which are 10 feet long, are marked in the 1.5-acre field. Images are collected during the harvest of these plots. The harvesting of the field took 2 days, during which the 37 10-feet plots were covered on the first day of harvest. Due to the weather and technical difficulties the number of usable plots reduced from 37 to 19.

Images of the 19 plots are processed, and information of the pixel area covered by the sweetpotatoes, the polar moment of inertia, width, height of the rectangle that can drawn around the detected sweetpotato and the length of the major and minor axes of the sweetpotato are extracted. The weight and size are estimated with the features of the detected sweetpotatoes as a training set. Compared to the graded sweetpotatoes, it is observed that the pixel area decreased due to the presence of mud on the surface of the sweetpotatoes. Little effect is observed on the remaining features. To overcome this problem, it is estimated that a 30% increase in the pixel area would compensate for the differences in pixel area between un-graded and graded data.

Apart from the weight and grade estimation, the total number of sweetpotatoes harvested from each plot is also calculated. Figure 6-8 shows a comparison of the actual number versus the predicted number. The resulting R^2 is calculated to be 0.80. The reasons for the system not being able to detect with 100% accuracy are: 1) due to the failure of detection of sweetpotatoes covered with mud, 2) some culls being discarded during harvest

but detected by the system and 3) failure in the image segmentation algorithm discussed in the starting of this chapter.

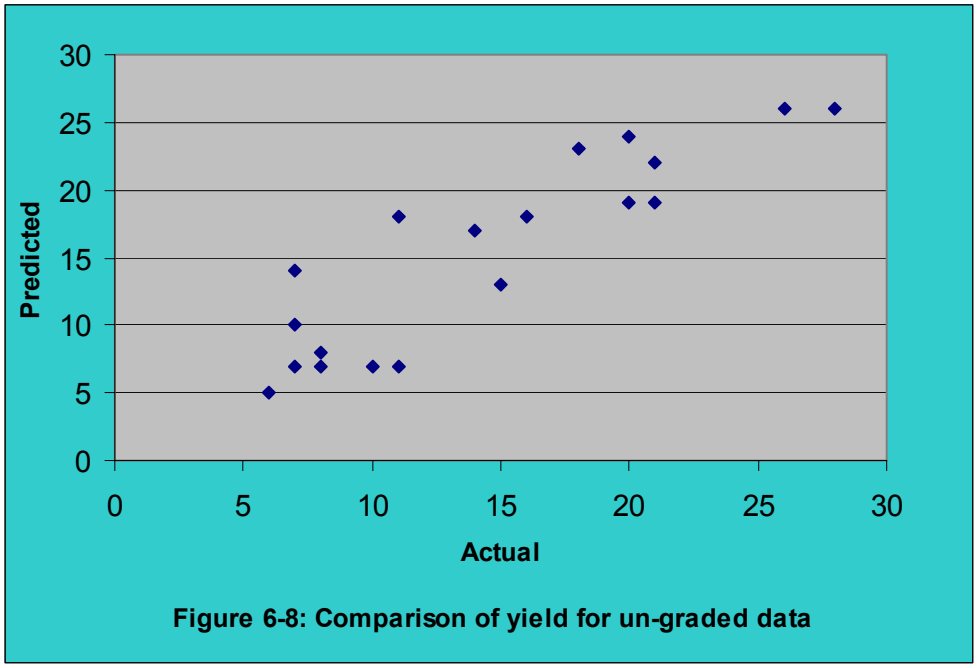

Figure 6-8: Comparison of yield for un-graded data

Weight Estimate

From both Figure 6-4 and Figure 6-5, it can be observed that classifier4 performs the best, and hence it is used in the evaluation of the weight estimate on the un-graded data. The weights of the sweetpotatoes are calculated in grams. The results of the predicted weight versus the actual weight are shown in Figures 6-9 and 6-10 respectively. Figure 6-9 shows the results of the performance with the REG procedure. Figure 6-10 shows the results of using neural networks with 10 hidden nodes and 4 output nodes. Both neural networks and statistical methods performed with a considerable accuracy of 88.4% and 84.8% respectively.

Due to the errors introduced in the detected number of sweetpotatoes in the 10-feet plots and the error in the weight analysis, the overall accuracy for un-graded data decreased compared to the graded data.

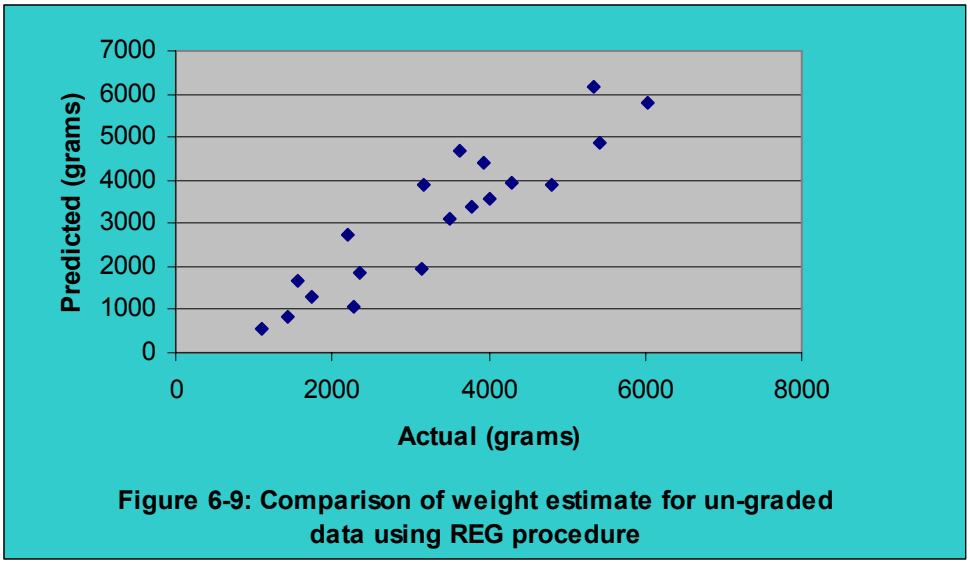

Figure 6-9: Comparison of weight estimate for un-graded data using REG procedure

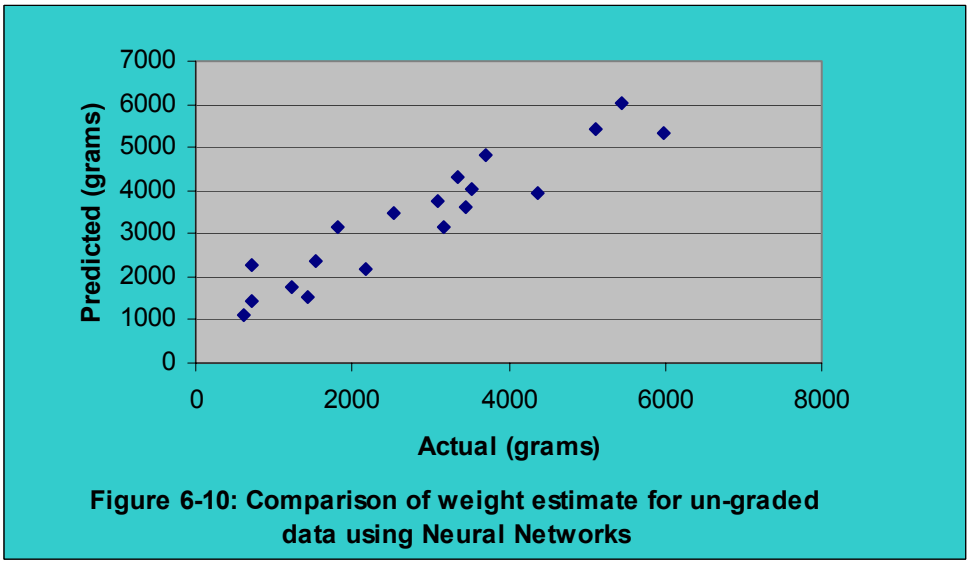

Figure 6-10: Comparison of weight estimate for un-graded data using Neural Networks

Grade Estimate

As mentioned in Section 2.1 sweetpotatoes are classified into 4 categories: culls, canners, U.S. No.1's, and jumbos. Grading of the sweetpotatoes is performed in a similar way to the weight estimate. Classifier4 with the highest accuracy is used for the evaluation of un-graded data. Results of the grade classification with discriminant analysis are shown in Table 6-3. Table 6-4 shows the grade classification with neural networks. Neural networks performed better than statistical methods. Maximum error is observed in grading culls. More culls were classified as canners and a few into U.S. No.1's. A few U.S. No.1's are graded as culls. Considering all the different grades, an R^2 of 0.316 is obtained with the DISCRIM procedure and 0.40 is obtained with neural networks. The accuracy rate is increased in neural networks when culls are not taken into consideration for estimating the performance of the system. An R^2 of 0.63 resulted from the use of neural networks and 0.616 is observed with the discriminant analysis in this scenario with the culls removed.

U.S. No.1's being the highest priced sweetpotatoes, evaluation of the accuracy in predicting their yield is performed. From the conducted experiments it can be concluded that in an acre with 25000 lbs yield of U.S. No.1's the accuracy is approximately within 4478 lbs with statistical method and within 1545 lbs with neural networks. Therefore it can be stated that the practical implementation of the system will provide considerable results with neural networks. Better results will be obtained if care is taken to prevent sweetpotatoes from being covered with huge lumps of mud as observed in a couple of 10-feet plots used for the evaluation.

Table 6-3: Performance comparison of grade estimate on un-graded data using DISCRIM procedure.

Plots	Actual				Predicted			
	Cull	Canner	U.S.No.1	Jumbo	Cull	Canner	U.S.No.1	Jumbo
11A	10	0	0	0	1	5	1	0
12A	3	11	7	0	0	16	5	1
12B	5	9	6	0	2	9	6	2
12C	11	1	3	0	2	5	6	0
13A	5	2	0	0	3	6	1	0
13B	4	11	3	0	6	12	5	0
13C	4	5	1	1	3	11	2	2
14B	2	0	5	0	3	6	5	0
14C	1	3	3	1	0	5	3	0
2A	8	10	3	0	7	11	1	0
2B	8	14	6	0	6	13	7	0
3A	15	7	4	0	3	13	8	2
3B	8	9	3	0	1	14	9	0
4A	2	10	4	0	0	10	8	0
4B	7	4	2	1	7	7	3	0
5A	2	1	5	0	1	3	3	0
5B	2	8	1	0	2	3	2	0
6A	5	2	0	0	0	6	1	0
7A	1	1	3	1	1	3	0	1

Table 6-4: Performance comparison of grade estimate on un-graded data using Neural Networks.

Plots	Actual				Predicted			
	Cull	Canner	U.S.No.1	Jumbo	Cull	Canner	U.S.No.1	Jumbo
11A	10	0	0	0	1	6	0	0
12A	3	11	7	0	2	19	1	0
12B	5	9	6	0	2	9	5	3
12C	11	1	3	0	3	5	3	2
13A	5	2	0	0	4	5	1	0
13B	4	11	3	0	8	10	5	0
13C	4	5	1	1	5	8	4	1
14B	2	0	5	0	5	3	6	0
14C	1	3	3	1	0	4	4	0
2A	8	10	3	0	9	9	1	0
2B	8	14	6	0	6	13	7	0
3A	15	7	4	0	5	11	7	3
3B	8	9	3	0	0	17	7	0
4A	2	10	4	0	2	9	7	0
4B	7	4	2	1	4	6	7	0
5A	2	1	5	0	0	2	4	1
5B	2	8	1	0	3	3	1	0
6A	5	2	0	0	0	7	0	0
7A	1	1	3	1	0	5	0	0

CHAPTER VII

CONCLUSIONS AND FUTURE WORK

Machine vision as an approach to yield monitoring of sweetpotatoes is effective. The developed system performed with considerably accuracy for weight estimations, but was not effective in grade estimations. The capability of neural networks to perform better in noisy data compared to traditional statistical methods has proven to be useful in obtaining higher accuracy. This chapter discusses results and includes suggestions for future work that will enhance the performance of the system.

7.1 Future Work

Detection of sweetpotatoes in the presence of mud is an area that requires further improvement. To overcome this problem, better algorithms can be developed that will use artificial intelligence or neural networks to detect the shape of the sweetpotatoes. An alternative approach is to use a rotating brush that can be placed on the conveyor belt ahead of the region where the camera is placed. The brush can be used to remove the mud present on sweetpotatoes moving up to the sorting area. Additional work is also required in developing a better lighting system.

For the purpose of the experiments, the speed of the conveyor belt is kept constant during the harvest. This is not the typical scenario in the field during harvest; the speed of

the conveyor belt increases or decreases with the number of people working in the sorting area and also with the number of sweetpotatoes that come up the conveyor belt. To utilize the system in realistic conditions, it is important to build a system that will control the speed of the camera according to the speed of the conveyor belt. If the speed of the conveyor belt is fed to the computer, the rate at which the frame grabber captures a frame can be altered accordingly.

7.2 Conclusions

A data acquisition system is built for yield monitoring of sweetpotatoes. An image segmentation algorithm to identify sweetpotatoes in images performs with an accuracy of 80%. Neural networks and statistics are also used to estimate the grade and weight of the sweetpotatoes. Neural networks performs with an R^2 value of 0.63 for grade analysis and with an R^2 of 0.884 in the weight analysis. An R^2 value of 0.616 was observed in grade analysis and an R^2 of 0.848 in weight analysis with statistical methods. Inclusion of additional information like width and length of the area covered by the sweetpotato and the length of the major and minor axes increased the accuracy rate for weight and grade estimation.

REFERENCES

[1] S.A. Shearer, S.G. McNeill, S.F. Higgins and R.I. Barnhisel, “Basics of Yield Monitoring”, Biosystems and Agricultural Engineering, University of Kentucky.

[2] “Cotton Yield Monitor”, Ag Leader Technology.

[3] J. A. Thomasson**,** J. G. White and P. G. Thompson**, “**Sweetpotato Yield Monitor Based on Optical Imaging Techniques” ASTA project report, 2000.

[4] http://www.redhorsetech.com/

[5] http://www.harvestmaster.com/

[6] J. R. Wooten, J. A. Thomasson, J. G. White and P. G. Thompson, "Yield and Quality Monitor for Sweetpotato with Machine Vision", ASAE Paper 001123. St. Joseph, Mich.: ASAE, 2000.

[7] Deck, S., C. T. Morrow, P. H. Heinemann, and H. J. Sommer, "Neural Networks for Automated Inspection of Produce", ASAE Paper No. 923594. St. Joseph, Mich.: ASAE, 1992.

[8] Alchanatis, V., and S. W. Searcy, "High Speed Inspection of Carrots with a Piplelined Image Processing System", ASAE Paper No. 953170. St. Joseph, Mich.: ASAE, 1995.

[9] Delwiche, M. J., S Tang, and J. F. Thompson, "A High Speed Sorting System for Dried Prunes", Trans. ASAE 36(1), pp. 195-200, 1993.

[10] Das, K., and M. D. Evans, "Image Processing Algorithms for Detecting Infertile Eggs during Early Incubation", ASAE Paper No. 917010. St. Joseph, Mich.: ASAE, 1991.

[11] Petterson, A., L. Olsson, and S. Lundqvist, "On-Line Measurement of Wood Chip Size", Tappi Journal, pp. 78-81, July 1988.

[12] R.C. Crida and G. de Jager, "Multiscalar Rock Recognition using Active Vision", IEEE International Conference on Image Processing, pp. 345-348, September 1996.

[13] R. C. Crida, "A Machine Vision Approach to Rock Fragmentation Analysis", PhD Thesis, University of Cape Town, 1995.

[14] R. G. Gonzalez and R. E. Woods, "Digital Image Processing", Addison-Wesley Publishing Company, 1993.

[15] Russ, John C, "The Image Processing Handbook", Boca Raton, Fla.: CRC Press, c1992.

[16] A. K. Jain, "Fundamental of Digital Image Processing", Prentice Hall Information and System Science Series, 1989.

[17] Pratt, William K, "Digital Image Processing", New York: Wiley, c1978.

[18] N. Mamoru and O. Takeshi, "Image processing method and apparatus for extracting lines from an image by using the Hough transform", U.S. Patent 5,832,138, 1998.

[19] Image Transforms - Hough Transform, http://cs-alb-pc3.massey.ac.nz/notes/59318/l11.html.

[20] Beer, F. P., and E.R. Johnston, Jr. "Mechanics of Material", New York: McGraw-Hill, 1981.

[21] Anonymous, "SAS/STAT User Guide", Release 6.03, Cary, N.C.: SAS Institute, 1988.

[22] Rudolf Jakob Freund, William J. Wilson, "Statistical Methods: Revised Edition", Academic Press, 1996

[23] Simon S. Haykin, "Neural Networks: A Comprehensive Foundation" 2nd edition. NJ: Prentice Hall, 1998.

[24] "Stuttgart Neural Network Simulator", Developed at University of Stuttgart

[25] MCI commands, Integral Flashbus Reference manual.

[26] Borland C++ Builder Guide, 5th edition, 2000.

[27] Color in Image and Video, http://www.cs.sfu.ca/CourseCentral/365/li/material/notes/Chap3/Chap3.3/Chap3.3.html

[28] Dana H. Ballard and Christopher M. Brown, "Computer Vision", Englewood Cliffs, N.J.: Prentice-Hall, c1982.

[29] M. Brady, "Computer Vision", Amsterdam : North-Holland Pub. Co., 1981.